

Influence of Lipid Membrane Rigidity on Properties of Supporting Polymer

Michael S. Jablin,[†] Manish Dubey,[†] Mikhail Zhernenkov,[†] Ryan Toomey,[‡] and Jarosław Majewski^{†*}

[†]Lujan Neutron Scattering Center, Los Alamos National Laboratory, Los Alamos, New Mexico; and [‡]Department of Chemical and Biomedical Engineering, University of South Florida, Tampa, Florida

ABSTRACT Temperature-sensitive hydrogel polymers are utilized as responsive layers in various applications. Although the polymer's native characteristics have been studied extensively, details concerning its properties during interaction with bio-related structures are lacking. This work investigates the interaction between a thermoresponsive polymer cushion and different lipid membrane capping layers probed by neutron reflectometry. *N*-isopropylacrylamide copolymerized with methacroylbenzophenone first supported a lipid bilayer composed of 1,2-dipalmitoyl-*sn*-glycero-3-phosphoethanolamine (DPPE) and subsequently 1,2-dipalmitoyl-*sn*-glycero-3-phosphocholine (DPPC). The polymer-membrane systems were investigated above and below the polymer transition temperature (37 and 25°C). Although the same cushion supported each lipid membrane, the polymer hydration profile and thickness were markedly different for DPPE and DPPC systems. Because DPPE and DPPC have different bending rigidities, these results establish that the polymer-membrane interaction is critically mediated by the mechanics of the membrane, providing better insight into cell-hydrogel interactions.

INTRODUCTION

Stimuli responsive polymers undergo structural changes in response to alterations in their environment. In particular, thermoresponsive polymers have gained attention due to their application in catalysis (1–3), drug delivery and release (4), and tissue engineering (5,6). Poly(*n*-isopropylacrylamide) (PNIPAAm), one such thermoresponsive polymer, exhibits a phase transition at 32°C and has been studied extensively since it was first reported 40 years ago (7). In response to small temperature variations, PNIPAAm radically changes its volume by expelling or uptaking water between its polymer chains. Although many proof-of-concept studies have utilized PNIPAAm, little is known about the polymer-system interaction in these applications (8).

One of the most promising applications of PNIPAAm is the controllable release of cultured cell sheets. PNIPAAm has been shown to be nontoxic and at physiological temperature (37°C) is collapsed, leading to successful cell adherence and growth (9). When temperature is reduced beneath the polymer transition temperature (~32°C), the cultured cells are released from the polymer matrix as an intact sheet due to the designed hydrophobicity of the underlying substrate. Although various PNIPAAm-modified surfaces have been evaluated, the mechanism regarding the temperature-controlled cell attachment and detachment remains unclear. It is believed that the hydration of the matrix plays an important role in determining the mechanism of cell attachment and detachment (10). The application of PNIPAAm is problematized by studies demonstrating that substrate mechanical properties (elasticity and rigidity) regulate the fate (cell shape, cytoskeletal rearrangement, tissue rigidity, signaling, differentiation,

stemness, and survival) of cultured cells (11). To combat this issue, the substrate's mechanical properties are determined before culturing cells. This practice assumes that the cell-substrate interaction does not alter substrate characteristics significantly. However, we report drastic changes in the characteristics of a PNIPAAm copolymer when it supports different surrogate lipid membranes.

There has also been an increased interest in the effect of matrix elasticity on cell lineage specification (12). Polymeric matrices with known stiffness are utilized as supports to understand the physical effects of in vivo tissue microenvironment for therapeutic uses of stem cells. It is believed that the stem cells sense the matrix elasticity and transduce this information into morphological changes. Although the effect of matrix elasticity on the proliferation of cells has been established, it is imperative to consider the changes induced in the matrix as a result of the immobilized cells. This study highlights the interplay between the immobilized cells and the underlying polymer. We report significant changes in the physical properties of the polymer substrate after being capped by different model lipid membranes. Although cell culture studies commonly are performed using micrometer-thick matrices, much thinner layers, such as used in this study, allow precise neutron reflectometry (NR) measurements of the polymer's hydration.

SAMPLE PREPARATION

1,2-Dipalmitoyl-*sn*-glycero-3-phosphoethanolamine (DPPE) and 1,2-dipalmitoyl-*sn*-glycero-3-phosphocholine (DPPC) were purchased from Avanti Polar Lipids (Alabaster, AL) and used without further purification (molecular structures shown in Fig. 1). Stock solutions of DPPE and DPPC were prepared by dissolution of chemicals in chloroform and methanol. Before depositing the lipids, a 3-inch

Submitted March 31, 2011, and accepted for publication May 25, 2011.

*Correspondence: jarek@lanl.gov

Editor: Ka Yee C. Lee.

© 2011 by the Biophysical Society
0006-3495/11/07/0128/6 \$2.00

doi: 10.1016/j.bpj.2011.05.054

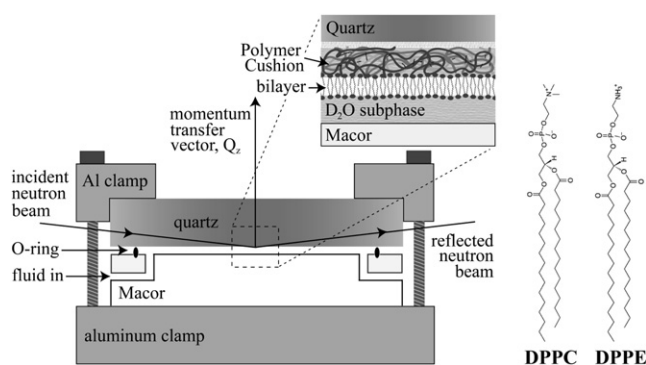


FIGURE 1 Schematic view of the solid-liquid interface cell. Before and after depositing a bilayer on top of the polymer cushion, the quartz substrate was clamped against a Macor (Ceramic Products) disk with a 0.2–0.3-mm-thick, subphase-filled gap created by an O-ring. The neutron beam penetrated the lateral face of the quartz substrate and was scattered from the solid-liquid interface. The molecular structure of DPPC and DPPE are shown to the right of the solid-liquid cell.

diameter quartz monocrystal (*c*-cut, α -quartz, density 2.64–2.65 g·cm⁻³, Institute of Electronic Materials Technology, Warsaw, Poland) was cleaned thoroughly by rinses alternating between chloroform, toluene, methanol, and high purity water (18 M Ω). Finally, the substrate was placed in an ultraviolet-ozone cleaner for 20 min. Then, the cleaned quartz substrate surface was modified with 3-amino-propyltriethoxysilane deposited from a 1% solution in acetone. The silane-coupling agent covalently bonds to the substrate and establishes a well-controlled and uniform surface against which the polymer cushion layer can be reproducibly anchored by van der Waals forces.

Finally, PNIPAAm copolymerized with methacroylbenzophenone (PNIPAAm-co-MaBP) was spin-coated on the quartz substrate and cross-polymerized using ultraviolet light (13,14). The lipid solutions were deposited by a microsyringe onto the air/water interface in a Langmuir trough (NIMA, Coventry, UK). At least 10 min were allowed for solvent evaporation, and then, the monolayers were compressed to a surface pressure of 40 mN/m. After film stabilization, the inner and outer membrane leaflets were transferred by the Langmuir-Blodgett and Langmuir-Schaefer techniques, respectively, onto the modified quartz substrate (15). The entire deposition was performed at 37°C. A control sample was prepared by spin-coating deuterated polystyrene on top of a poly(*n*-propylacrylamide) copolymer cushion.

The polymer and polymer-supported membranes were measured in a solid-liquid interface cell (Fig. 1). The setup was composed of the quartz substrate supported by an O-ring and a Macor ceramic disk (Ceramic Products, Palisade Park, NJ). The Macor, O-ring, and substrate define a 0.2–0.3-mm thick reservoir for the subphase. The entire sample environment was held in place with aluminum clamps. Neutrons entered the lateral face of the quartz substrate and were scattered from the quartz-subphase inter-

face. The native polymer and polymer-supported bilayers were characterized against a subphase of D₂O above and below the polymer transition temperature (37 and 25°C). Although PNIPAAm's phase transition temperature in D₂O is 1°C higher (~33°C) than in H₂O (16), the temperatures used in this study (25°C and 37°C) are far from these critical temperatures, greatly diminishing the effect of isotopic substitution on the polymer's attributes. D₂O provided neutron scattering contrast among quartz, the hydrogen-rich bilayer, the polymer, and the subphase. Considering the deposition surface pressure and measured temperature range, both DPPE and DPPC membranes are consistently below their main transition temperature. Additionally, the surface coverage of the bilayers was similar.

NEUTRON REFLECTOMETRY

Because neutrons are only scattered by nuclei, they penetrate sample environments to assess buried interfaces, and therefore, NR is frequently utilized to probe biological structures in aqueous environments (17,18). NR experiments were performed on the Surface Profile Analysis Reflectometer (SPEAR), a time-of-flight reflectometer at the Los Alamos National Laboratory Lujan Neutron Scattering Center. SPEAR (<http://www.lansce.lanl.gov/lujan/instruments/SPEAR/index.html>) receives neutrons from a polychromatic, pulsed (20 Hz) source that pass through a partially coupled liquid hydrogen moderator at 20 K to shift their energy spectrum. Choppers and frame-overlap mirrors reduce the wavelength range of the neutrons to 2–16 Å. The wavelength, λ , and momentum of incident neutrons are related by the de Broglie relation, $\lambda = hp^{-1}$, where h is Planck's constant and p is the momentum of the neutron. By measuring the time it takes a neutron to travel the length of the instrument, the neutron's momentum—and therefore its wavelength—can be determined.

During an NR experiment, neutrons impinge on a sample at a small angle, θ , and the ratio of elastically scattered/incident neutrons is measured. This ratio is defined as the reflectivity, R , and is measured as a function of the momentum transfer vector, Q_z , where $Q_z = 4\pi\sin[\theta]\lambda^{-1}$. Neutrons are reflected and refracted from changes in scattering contrast within the system and constructively and destructively interfere, creating a characteristic series of minima and maxima (i.e., Kiessig fringes) in the measured reflectivity profile. The incident neutron beam is collimated with a series of slits to create a footprint on the sample of $\sim 20 \times 50$ mm. The coherent area of the neutron beam projected onto the sample is ~ 10 nm \times 100 μ m, and the acquired data are an average of the reflectivity from each coherent area that makes up the footprint.

Analysis of specular reflectometry data provides information regarding the coherent scattering length density (SLD) distribution normal to a sample's surface, SLD(z), where z denotes distance from the substrate. SLD is a value unique

to a particular chemical composition and is the sum of the coherent scattering lengths of the constituent elements, divided by the volume they occupy. It is important to note that the measured SLD values are absolute because NR data are normalized to the incident neutron intensity. To obtain a real-space interpretation of the scattering data, $SLD(z)$, a Fourier transform, can be applied. Because only intensity and no phase information is collected, a unique Fourier transform between a single NR profile and its real-space interpretation does not exist. Therefore, modeling was employed to interpret the NR data.

The continuous function $SLD(z)$ often can be well approximated by a number of layers, referred to as boxes, each with a constant SLD. Interlayer roughness can be taken into account using an error function centered at each interface (19). The incident neutron beam is refracted at each interface, and a theoretical NR curve can be calculated using the Parratt recursion formula (20). The measured and theoretical NR curves are compared, and by using genetic optimization and the Levenberg-Marquardt nonlinear least-squares method, the best least-squares fit, corresponding to the lowest χ^2 value, is obtained (21). Although a large number of boxes can be used to approximate the true SLD distribution, a system easily can become overparameterized. To ensure that our measured systems were not overparameterized, we utilized the simplest (fewest-boxes) model of physical relevance.

DATA FITTING PHILOSOPHY

The thickness and SLD of the native polymer cushion was determined before membrane deposition. The cushion was characterized by NR in air and in D_2O at 37 and 25°C. Using these measurements, the SLD of the dry polymer (SLD_{poly}) and the mass of polymer on the surface were determined. Conserving polymer mass was an important criterion for fitting the scattering from the polymer-membrane systems. A value proportional to polymer mass can be calculated using

$$\text{Polymer Amount} \propto \int_{z_1}^{z_2} \varphi(z) dz = \int_{z_1}^{z_2} \frac{SLD(z) - SLD_{D_2O}}{SLD_{poly} - SLD_{D_2O}} dz,$$

where z is the depth from the quartz substrate surface, $\varphi(z)$ is the volume fraction polymer, $SLD(z)$ is the SLD distribution, and z_1 and z_2 define the boundaries of the polymer region.

First, the native properties of PNIPAAm-co-MaBP were determined. Subsequently, a membrane composed of DPPE was deposited onto PNIPAAm-co-MaBP and the polymer-DPPE system was investigated. Then, DPPE was removed from the polymer surface by chloroform and ethanol rinses, and the polymer was measured to reestablish its stability. Finally, a DPPC membrane was deposited onto the same cushion, and the polymer-DPPC system was

studied. Using the above equation, the volume fraction of D_2O was calculated. This calculation is strictly valid within the PNIPAAm-co-MaBP region and is an approximation at the quartz-polymer and polymer-membrane interfaces.

RESULTS AND DISCUSSION

Instead of live cells, DPPC and DPPE were studied because they exhibit similar bilayer properties when deposited by Langmuir-Blodgett/Langmuir-Schaefer and measured by NR (thickness, density, coverage, etc.). However, they have significantly different mechanical properties (bending rigidity) due primarily to their different headgroups. The molecularly different headgroups result in different packing, which is likely the main reason for the difference in their mechanical properties. Apart from these considerations, understanding the membrane-substrate interaction, especially the hydration of the underlying polymer, also has been shown to be important in the study of supported bilayers (22).

The polymer-bilayer systems were characterized above and below the polymer transition temperature. First, the results of the neutron scattering from the polymer-membrane systems are compared at 37°C when PNIPAAm-co-MaBP was collapsed (Fig. 2 a). Although the thickness of the polymer was nearly the same irrespective of capping lipid membrane composition, radically different polymer hydration profiles were measured (Fig. 3, a and b). The thickness of the polymer when it supported DPPE versus DPPC can be judged directly from the NR data. The first several minima of the DPPE and DPPC NR data are consistent, strongly suggesting very similar thicknesses. From the relative intensity of the NR data, the hydration also is apparent. When it supports DPPE, the polymer is more hydrated.

Because the subphase is D_2O ($SLD_{D_2O} = 6.33 \times 10^{-6} \text{ \AA}^{-2}$), there is greater SLD contrast between the hydrated polymer and the hydrogenated bilayer ($SLD_{bilayer} \sim 0 \times 10^{-6} \text{ \AA}^{-2}$), which results in increased intensity. In the DPPE case (Fig. 3 b), the polymer had a very steep hydration gradient, rapidly transitioning from 50 to >90 volume % water in the

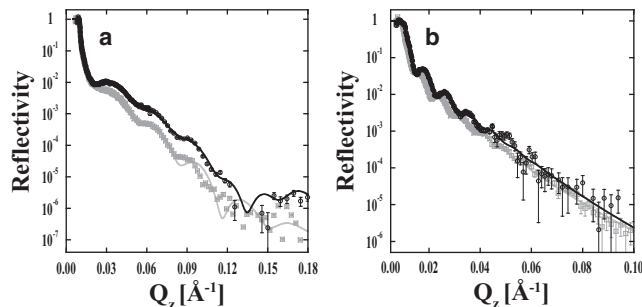


FIGURE 2 Measured scattering from bilayers supported by PNIPAAm-co-MaBP at 37°C (a) and 25°C (b). Shown are the NR data of polymer-DPPE (open circles) and polymer-DPPC (open squares) with corresponding fits shown by solid and shaded lines, respectively. The error bars indicate 1 SD.

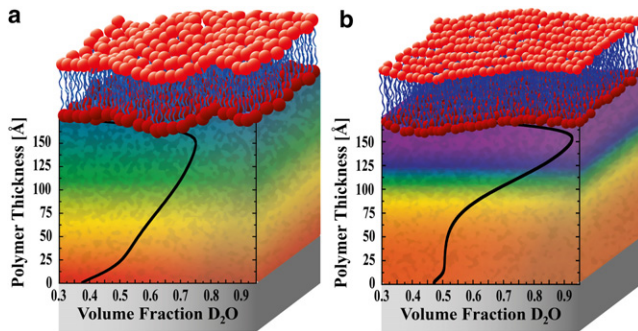


FIGURE 3 Polymer hydration profiles when it supported DPPE (*a*) and DPPC (*b*) model membranes at 37°C. The polymer is supported on a quartz substrate (depicted by *shaded boxes*). The color gradient in the polymer region is drawn as a guide to the eye and corresponds to the overlaid hydration profile.

direction away from the quartz substrate (0–150 Å). In contrast, when the polymer supported DPPC (Fig. 3 *a*), the hydration profile shows an approximately linear increase in water volume fraction. The artificial decrease in water volume fraction when the hydration profiles approach the position of the membrane (beyond 150 Å) is due to 1), the condition that, within the membrane, the water volume fraction must be zero; and 2), the nonzero root mean-square roughness on the polymer-membrane interface used in the model.

Next, NR results from polymer-DPPE and -DPPC systems are examined at 25°C when the polymer had a greater average water volume fraction and therefore was swollen (Fig. 2 *b*). Despite the fact that DPPE and DPPC were supported by the same polymer, PNPAAm-co-MaBP extends ~10% farther when it supported DPPC as opposed to the case of DPPE (Fig. 4). The polymer-DPPC system is clearly thicker because the minima in its NR profile are shifted to lower Q_z values relative to the minima of the DPPE system. As also observed at 37°C, the polymer's hydration profile is sensitive to the composition of the supported membrane, but the profiles are significantly more uniform in both cases at 25°C (Fig. 4).

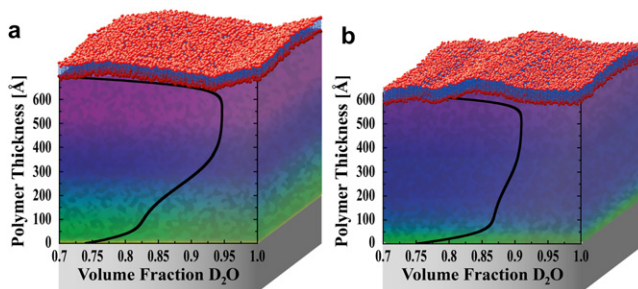


FIGURE 4 Polymer hydration profiles when it supported DPPC (*a*) and DPPE (*b*) model membranes at 25°C. The polymer is supported on a quartz substrate (depicted by *shaded boxes*). The color gradient in the polymer region is drawn as a guide to the eye and corresponds to the overlaid hydration profile.

After the reduction of temperature to 25°C, neutron scattering was collected from both polymer-DPPE and -DPPC systems once again at 37°C to establish the reproducibility of the polymer's hydration (Fig. 5 *a*). Comparison of the two 37°C polymer-membrane NR measurements demonstrates the reproducibility of the system. Both the position of the minima and the intensity (which is sensitive to hydration) are consistent. Additionally, the structure of the PNPAAm-co-MaBP cushion was reestablished after removing the DPPE membrane but before depositing the DPPC bilayer (Fig. 5 *b*).

Although a polymer-membrane interaction was expected, the degree to which their interaction affects PNPAAm-co-MaBP's hydration is nevertheless surprising. The lipid membrane is not covalently bound to its supporting polymer. Instead, only a weak van der Waals interaction keeps the membrane atop its cushion (23–25). Both membranes were supported by the same cushion, which strongly suggests that the water distribution within the polymer is critically sensitive to membrane properties. Although DPPE and DPPC are molecularly similar (identical saturated acyl tails), their headgroups differ in size and composition (ethanolamine is smaller than phosphocholine). DPPE's smaller headgroup facilitates a more comprehensive tail-tail interaction, which is manifested macroscopically in a greater bending rigidity for DPPE as compared to DPPC.

The polymer hydration also was measured when a substantially rigid system (180 Å thick deuterated polystyrene (dPS) layer spin-coated on a poly(*n*-propylacrylamide) (PNPAAm) copolymer) was employed. In this case, PNPAAm-co-MaBP was determined to be completely temperature-insensitive (Fig. 6). At both temperatures, the thickness of PNPAAm was ~150 Å, with a hydration of ~25 vol %. The roughness of the PNPAAm/dPS interface

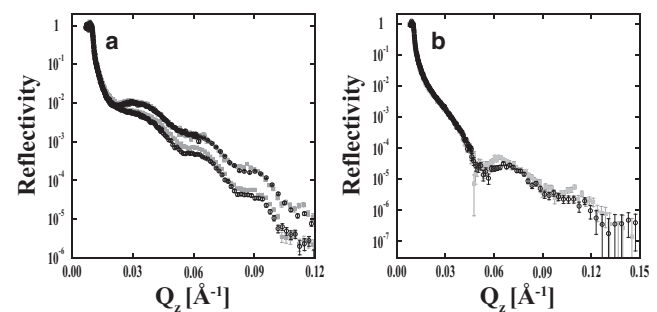


FIGURE 5 (*a*) NR measurements of polymer-DPPE (*upper two NR profiles*) and polymer-DPPC (*lower two profiles*) at 37°C before (*open circles*) and after (*shaded squares*) a temperature cycle down to 25°C. The consistency of the measurements emphasizes the reproducibility of the polymer-bilayer structures. (*b*) NR data from PNPAAm-co-MaBP in D₂O at 37°C. The NR data of the polymer are depicted before depositing DPPE (*open circles*) and after removing DPPE but before depositing DPPC (*shaded squares*). The consistency of the measurements shows that the polymer structure was unaltered by depositing or removing DPPE. Error bars indicate 1 SD.

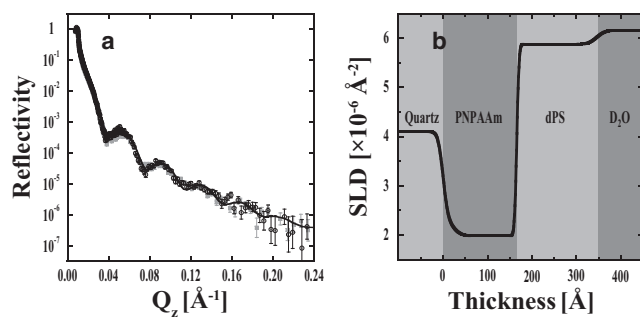


FIGURE 6 NR measurements of polymer-dPS in D₂O at 37°C (*open circles*) and 25°C (*shaded squares*). A single fit (*a*) and corresponding SLD profile (*b*) are shown (*solid line*). The consistency of the NR data indicates that the PNPAAm-co-MaBP shows significantly reduced temperature sensitivity when capped by a rigid dPS layer.

was small, which suggests minimal interpenetration of the layers. The nonzero water volume fraction of the PNPAAm cushion demonstrates that the dPS layer was water-permeable. This indicates that the polymer hydration is governed by the rigidity of the capping layer.

It previously has been reported that unconstrained PNIPAAm-co-MaBP expands isotropically upon temperature reduction. In contrast, the polymer's expansion is frustrated when it is chemically bound to a rigid substrate; it swells predominantly in the direction perpendicular to the substrate surface and to a much smaller extent in the direction parallel to the substrate (13,14). In addition to the anisotropic expansion, the total polymer volume change is significantly reduced when it is constrained. A capping lipid membrane is an additional constraint to polymer expansion. In the limit of an unextendable capping layer, the polymer's expansion will be suppressed almost completely in the direction parallel to the substrate surface, and therefore decreased in the direction normal to the substrate. The aforementioned extreme case was observed for a dPS capping layer. At 25°C, the polymer thickness is smaller when it supports DPPE as compared to DPPC, because DPPC is less rigid.

The hydration profile differences are linked to the lipid membrane mechanical properties. At 37°C, the polymer collapsed thickness is the same for both DPPE and DPPC cases, but the polymer hydration profiles are markedly different. The polymer can hydrate more uniformly when it is less influenced by the capping layer, which is the case for DPPC. When more constrained by DPPE, the hydration profile is more lopsided. The polymer hydration profiles can only be compared qualitatively at 25°C because the polymer thickness is different.

CONCLUSIONS

There is increased interest in understanding how cells respond to mechanical cues. PNIPAAm and its derivatives are used ubiquitously as substrates in biological studies

due to their thermoresponsive property; however, most of these cultured cell studies continue to assume that the cells do not perturb the properties of the substrate. It is well established that substratum properties significantly affect cell behavior. This study is an effort to understand how immobilized cells with different mechanical properties may influence the underlying polymeric substrate. NR experiments involving live cells adhered to a polymer layer are difficult to perform and interpret due to the complexity of the system. Therefore, two model lipid bilayers with different mechanical properties were studied instead.

The results of this study clearly demonstrate how a capping layer (model lipid membranes and polystyrene) affects the mechanical properties (hydration, swelling, and rigidity) of a supporting thermoresponsive polymer. Therefore, it is imperative that the mutual substrate-capping layer interaction be carefully considered when interpreting past and future cultured cell studies. Additionally, the polymer hydration profiles obtained from these experiments also provide valuable information for understanding the mechanism of attachment and detachment of cell sheets.

This work benefited from the use of the Lujan Neutron Scattering Center at the Los Alamos Neutron Science Center funded by the Department of Energy Office of Basic Energy Sciences and the Los Alamos National Laboratory under Department of Energy contract DE-AC52-06NA25396.

REFERENCES

- Bergbreiter, D. E., B. L. Case, ..., J. W. Caraway. 1998. Poly(*n*-isopropylacrylamide) soluble polymer supports in catalysis and synthesis. *Macromolecules*. 31:6053–6062.
- Hamamoto, H., Y. Suzuki, ..., S. Ikegami. 2005. A recyclable catalytic system based on a temperature-responsive catalyst. *Angew. Chem. Int. Ed. Engl.* 44:4536–4538.
- Ikegami, S., and H. Hamamoto. 2009. Novel recycling system for organic synthesis via designer polymer-gel catalysts. *Chem. Rev.* 109:583–593.
- Urry, D. W. 1992. Free energy transduction in polypeptides and proteins based on inverse temperature transitions. *Prog. Biophys. Mol. Biol.* 57:23–57.
- Akiyama, Y., A. Kikuchi, ..., T. Okano. 2004. Ultrathin poly(*n*-isopropylacrylamide) grafted layer on polystyrene surfaces for cell adhesion/detachment control. *Langmuir*. 20:5506–5511.
- Chan, G., and D. J. Mooney. 2008. New materials for tissue engineering: towards greater control over the biological response. *Trends Biotechnol.* 26:382–392.
- Heskins, M., and J. E. Gillet. 1968. Solution properties of poly(*n*-isopropylacrylamide). *J. Macromol. Sci. Chem.* A2:1441.
- Pelton, R. 2000. Temperature-sensitive aqueous microgels. *Adv. Colloid Interface Sci.* 85:1–33.
- Takezawa, T., Y. Mori, and K. Yoshizato. 1990. Cell culture on a thermo-responsive polymer surface. *Biotechnology (N. Y.)*. 8:854–856.
- Fukumori, K., Y. Akiyama, ..., T. Okano. 2010. Characterization of ultra-thin temperature-responsive polymer layer and its polymer thickness dependency on cell attachment/detachment properties. *Macromol. Biosci.* 10:1117–1129.
- Gilbert, P. M., K. L. Havenstrite, ..., H. M. Blau. 2010. Substrate elasticity regulates skeletal muscle stem cell self-renewal in culture. *Science Expr.* 101126/science.1191035.

12. Engler, A. J., S. Sen, ..., D. E. Discher. 2006. Matrix elasticity directs stem cell lineage specification. *Cell*. 126:677–689.
13. Vidyasagar, A., J. Majewski, and R. Toomey. 2008. Temperature induced volume-phase transitions in surface-tethered poly(*n*-isopropylacrylamide) networks. *Macromolecules*. 41:919–924.
14. Vidyasagar, A., H. L. Smith, ..., R. G. Toomey. 2009. Continuous and discontinuous volume-phase transitions in surface-tethered, photo-crosslinked poly(*n*-isopropylacrylamide) networks. *Soft Matter*. 5:4733–4738.
15. Smith, H. L., M. S. Jablin, ..., J. Majewski. 2009. Model lipid membranes on a tunable polymer cushion. *Phys. Rev. Lett.* 102:228102.
16. Milewska, A., J. Szydłowski, and L. P. N. Rebelo. 2003. Viscosity and ultrasonic studies of poly(*n*-isopropylacrylamide)-water solutions. *J. Polym. Sci. Pol. Phys.* 41:1219–1233.
17. Fragneto-Cusani, G. 2001. Neutron reflectivity at the solid/liquid interface: examples of applications in biophysics. *J. Phys. Condens. Matter*. 13:4973–4989.
18. Krueger, S. 2001. Neutron reflection from interfaces with biological and biomimetic materials. *Curr. Opin. Colloid Interf. Sci.* 6:111–117.
19. Nevot, L., and P. Croce. 1980. Characterization of surfaces by grazing x-ray reflection—application to study of polishing of some silicate-glasses. *Rev. Phys. Appl. (Fr.)*. 15:761–779.
20. Parratt, L. G. 1954. Surface studies of solids by total reflection of x-rays. *Phys. Rev.* 95:359–369.
21. Nelson, A. 2006. Co-refinement of multiple-contrast neutron/x-ray reflectivity data using MOTOFIT. *J. Appl. Crystallogr.* 39:273–276.
22. Seitz, P. C., M. D. Reif, ..., M. Tanaka. 2009. Modulation of substrate-membrane interactions by linear poly(2-methyl-2-oxazoline) spacers revealed by x-ray reflectivity and ellipsometry. *ChemPhysChem*. 10:2876–2883.
23. Israelachvili, J. N. 1992. Intermolecular and Surface Forces. Academic Press, London, UK.
24. Kaufmann, M., Y. F. Jia, ..., T. Pompe. 2011. Weakly coupled lipid bilayer membranes on multistimuli-responsive poly(*n*-isopropylacrylamide) copolymer cushions. *Langmuir*. 27:513–516.
25. Jablin, M. S., M. Zhernenkov, ..., J. Majewski. 2011. In-plane correlations in a polymer-supported lipid membrane measured by off-specular neutron scattering. *Phys. Rev. Lett.* 106:138101.